

# SYNCHRONOUS REFERENCE FRAME MULTILOOP CONTROL STRATEGY FOR A PV FED SINGLE-PHASE INVERTER

Nitin S

Assistant Professor, Universal Engineering College, Thrissur  
ntnsiva@gmail.com

**Abstract**—This paper proposes a Synchronous Reference Frame based multiloop control strategy for single-phase inverter fed from a photovoltaic system. The power electronic interface required for interfacing a photovoltaic module to a single-phase inverter is designed. The existing synchronous reference frame control for three phase systems is exploited to develop a closed loop control for single phase inverter. Here an inner capacitor current shaping along with an outersynchronous reference frame proportional integral (SRFPI) control is employed to attain performance of inverter with almost zero steady state error. A Matlab simulation model is presented with the results to justify the proposed work.

**Keywords**—Synchronous Reference Frame (SRF), Pulse Width Modulation (PWM), Microcontroller (MUC), All Pass Filter (APF), Voltage Source Inverter (VSI).

## I. INTRODUCTION

Rapid depletion of conventional energy sources and emerging environmental concern has induced a fast increase in the distributed generation especially from solar and wind resources. [1] Energy extracted from solar energy has dramatically increased by over 25 % in the past two decades accounting to the availability and reduction in prices of solar panels. [2] Attaining higher efficiencies from solar panels and novel manufacturing technologies has mainly attributed to this. The drawback, however lie in the intermittent energy supply from the renewable sources and lack of efficient control schemes to extract maximum power. Efficient power extraction needs power electronic devices to supply to grid and individual loads. [3]– [4]. In general a voltage source inverter (VSI) is used to work in both standalone and grid connected modes. While operating in the standalone mode and in applications involving critical loads, it is required to feed a controlled and high quality power. Thus the vital requirement is to control the system voltage constraints like amplitude and frequency with

quicker and efficient dynamic response and minimal steady-state error.

Numerous control strategies to operate the single phase VSI in standalone mode of operation are proposed in literature. Significant developments include the repetitive control [5], dead-beat control [6], and discrete-time sliding-mode control.[7]– [8] The repetitive control is more advanced and found to be efficient in eliminating the periodic load disturbances, but they have slower response and require constant tracking of the load variation. The dead-beat control, in spite of its inherent faster response is more sensitive to the system parameter variations and uncertainties due of its high gain. [6] The sliding mode is superior with respect to its robustness, stability and good regulation, but it suffers from power losses and severe electromagnetic compatibility noise. [8] The synchronous reference frame proportional integral controller is being used for three phase VSI, but its application in single phase converters is limited. Moreover these controllers are used in the grid connection and vector control of machines.

The main challenge in the implementation of the synchronous reference (DQ) frame controller for single phase systems is to obtain the orthogonal signal so as to perform park's transformation. Various techniques to generate the signal include use of a transfer delay [9], and various transformations on existing signals like Hilbert's transform [11], differentiated model [10], and Kalman's filter method [12]. The technique used here is the All Pass Filter (APF) method [13].

This paper focuses on the use of synchronous reference frame controller for single phase standalone systems and uninterrupted power supplies (UPS) applications. This paper presents a

multiloop control strategy for a sinusoidal PWM inverter to achieve instantaneous output voltage control, and improved transient and steady state performance. In the inner capacitor current loop, the current in the filter capacitor is used as the feedback variable. This enables to achieve a sinusoidal capacitor current and active damping of LC filter. An outer feed forward voltage control loop is included for load voltage regulation and correction of the imperfections in the inner current loop implementation.

The paper is organized as follows: Section II explain block diagram for operation of the system. Section II and III gives the design of the photovoltaic array and boost converter. Section VI explains the proposed system operation with a simulation. Section VII explains the control structure employed. Results of the matlab simulation are given in Section IV.

## II. BLOCK DIAGRAM

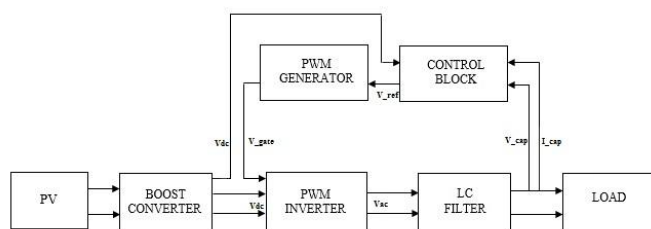


Fig. 1. Block diagram of Grid connected PV system

The basic block diagram representation of the proposed system is given in fig. 1. It is divided into following blocks or subsystems.

### A. PHOTOVOLTAIC SYSTEM

This block represents the model of a photovoltaic array. It is modeled considering the behavior of an actual solar cell to the physical environmental variables of available solar radiation and the ambient atmospheric temperature. The behavior of the array is modeled using the equations which relate the current output of the array with these variables. The equations also take into consideration the number of series and parallel connected cells which can be set to make the photovoltaic array deliver the required power. [14]

### B. DC-DC BOOST CONVERTER

The boost converter regulates the average output DC voltage at a higher level compared to the input voltage. Hence it is referred as a step-up converter. Due to the presence of an inductor of large value in series, it acts as a current source. [15] The parallel connected switch is turn on and off at a frequency such that the average value of output is greater than the input.

### C. SINUSOIDAL PULSE WIDTH MODULATION INVERTER

An inverter is a circuit in which the power given in DC form is converted to AC form. The sinusoidal pulse width modulation inverter used here is an H-Bridge inverter. It consists of 4 switches in two legs. The switches are triggered in such a manner that two switches in one leg never conduct simultaneously. The gating pulse to the inverter is given by a PWM generator. The output of the inverter depends on the pulse width of the firing pulses, thus it is called as pulse width modulated inverter.

### D. PWM GENERATOR

This block supplies the gating pulses for the H-Bridge inverter. The pulse generation principle adopted here is the sinusoidal pulse width modulation. In this technique the gating pulses for the inverter is produced by comparing a sinusoidal reference wave with a carrier triangular pulse sequence [16]. The amplitude of the sinusoidal reference is limited by the modulation index, which is the ratio of the magnitude of sine wave to the carrier wave magnitude. The output of the comparison is the square pulses whose pulse width varies with the sine wave [17]. The pulse width is high corresponding to the maximum amplitude of sine wave and vice versa.

### E. CONTROL BLOCK

Here the control is implemented so that the inverter compensates for the power from grid. The parameters sensed by the control block are output current of the grid and inverter and the output voltage of inverter. Whenever there is a change in the load values the current drawn by the load varies. This causes a relative error between the inverter and the grid currents. This condition is sensed by the control block and it varies the reference signal given as its output to the PWM generator. As a result the

pulse width of the resultant gating pulse and hence the output of inverter changes such that the extra power required by load is fed by the inverter.

### III. PHOTOVOLTAIC SYSTEM

The matlab model of photovoltaic array unit is given in fig. 2.

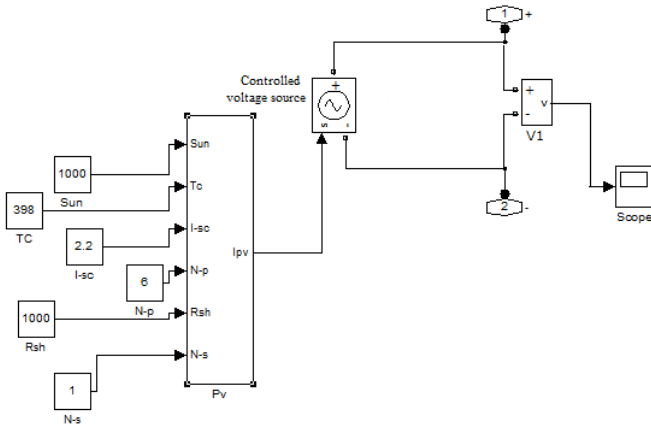


Fig. 2. Photovoltaic array

The equivalent model of the PV array is shown in “fig. 3” below.

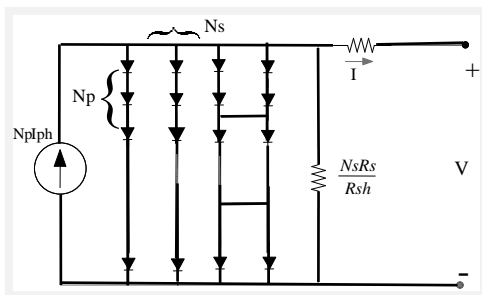


Fig. 3. Equivalent model of PV array

From the model it is evident that the number of cells connected in series and parallel is  $N_s$  and  $N_p$  respectively. In view of this the current to the load ( $I$ ) is given by expression (1).

$$I = N_p I_{ph} - N_p I_s \left[ \exp \left( \frac{q(V/N_s + I R_s / N_p)}{k T_c} \right) - 1 \right] - \frac{N_p V / N_s + I R_s}{R_{sh}} \quad (1)$$

The main parameters regarding the operation of a solar array are the diode photocurrent ( $I_{ph}$ ) and the saturation current ( $I_s$ ). Here the  $I_{ph}$  is the diode photo current which is derived from the solar irradiation given in (2).

$$I_{ph} = [I_{sc} + K_I (T_c - T_{ref})] * H \quad (2)$$

The saturation current ( $I_s$ ) is given by (3)

$$I_s = I_{RS} \left[ \frac{T_c}{T_{ref}} \right]^3 * \exp \left[ \frac{-q E_g (T_c - T_{ref})}{T_{ref} T_c k A} \right] \quad (3)$$

Where

$$I_{RS} = I_{sc} / \exp[V_{oc} / V_t] \quad (4)$$

$$V_t = (N_s K T_c A) / q \quad (5)$$

Where

$I_{ph}$  is a light-generated current or photocurrent,  $I_s$  is the cell saturation of dark current,  $q$  ( $= 1.6 \times 10^{-19}$  C) is an electron charge,  $K$  ( $= 1.38 \times 10^{-23}$  J/K) is a Boltzmann’s constant,  $T_c$  is the cell’s working temperature,  $A$  is an ideal factor,  $R_{sh}$  is a Shunt resistance,  $R_s$  is the series resistance of solar cell,  $N_p$  is no of parallel units,  $N_s$  is no of series units,  $I_{sc}$  is the cell’s short-circuit current at a  $25^\circ\text{C}$  and  $1\text{kW/m}^2$ ,  $K_I$  is the cell’s short-circuit current temperature coefficient,  $T_{ref}$  is the cell’s reference temperature,  $H$  is the solar insolation in  $\text{kW/m}^2$ ,  $I_{RS}$  is the cell’s reverse saturation current,  $V_{oc}$  is open circuit voltage of cell,  $V_t$  is the thermal voltage,  $E_g$  is the energy gap.

### IV. BOOST CONVERTER

The boost converter employed here to boost the voltage from 250 volt at the output of the photovoltaic array to a voltage of 500 volt. The switching frequency employed is 25 kHz. The output current is obtained a 20Amp. The value of the capacitor and inductor are obtained from the following equations (6) and (7).

$$C = \frac{I_{out} \cdot D}{\Delta V_{out} \cdot f_{sw}} \quad (6)$$

$$L = \frac{V_{in} \cdot D}{\Delta I \cdot f_{sw}} \quad (7)$$

Where

- $V_{in}$  – Input Dc voltage
- $D$  – Duty cycle.
- $\Delta i$  – 5% of output current.
- $f_{sw}$  – Switching frequency.
- $I_{out}$  – Output current.
- $\Delta V_{out}$  – 5% of output voltage.

### V. SYSTEM SIMULATION

The matlab model for the control of single phase inverter is shown in the fig. 4. The system parameters for simulation are given in table. 1. The inverter operates with the input output of the boost converter connected to the photovoltaic array.

Parameter	Value
Switching frequency	20 KHz
Fundamental frequency, $\omega_f$	$2\pi \times 50$ Krad/s
Filter Inductance, L	500 $\mu$ H
Filter Capacitance, C	22 $\mu$ F
ESR of Inductance, r	0.2 $\Omega$
Dc link voltage	48 V

Table. 1- Simulation parameters

A fixed Dc sources is used in the simulation model as input to the inverter. The H bridge inverter is used which derives the gating pulses from the synchronous reference frame controller. The controller operates upon the capacitor current and line voltage input from the LC filter applied at the output of the inverter. The capacitor current is sensed in the inner control loop to maintain a

sinusoidal current output. The design of the inner control loop lies in determining the gain K applied to the error current which is generated by comparing the actual capacitor current with the reference current generated from outer loop. The outer control loop takes the inverter line voltage as input. The voltage should be converted to synchronous reference frame by the Park's transformation. This demands a secondary orthogonal signal to be produced from the original voltage signal. To create an orthogonal signal from an original single-phase signal, different techniques have been proposed in the literature including the transfer delay block method, differentiating the original signal, Hilbert-transform, all-pass filter (APF). The all-pass filter (APF) is chosen in this study because it can be realised with much ease and it does not affect the higher order frequencies. The structure of a first order APF is shown in Fig. 2. The transfer function of APF structure is shown in (8), where  $\omega_f$  is the fundamental angular frequency

$$\frac{\omega_\beta(s)}{\omega_\alpha(s)} = \frac{\omega_f - s}{\omega_f + s} \quad (8)$$

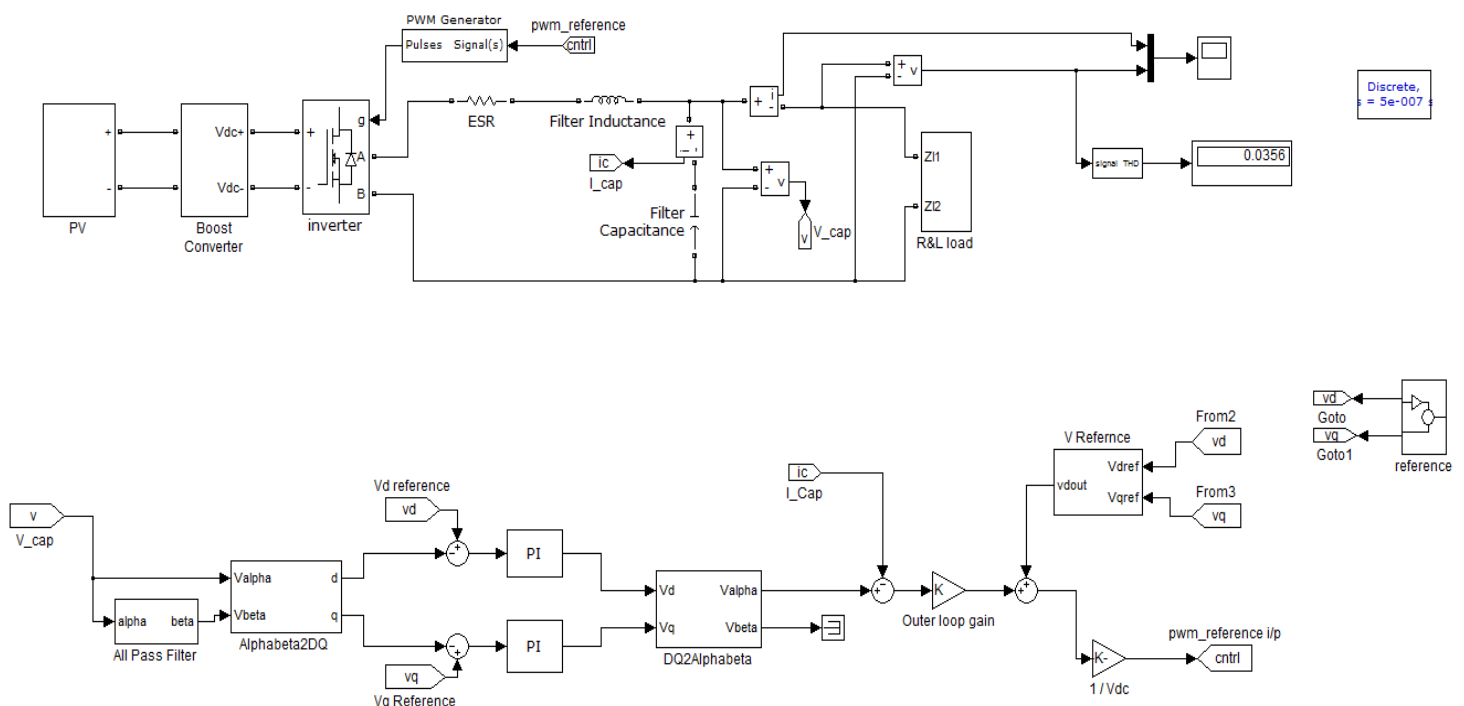


Fig. 4 – Simulation model of the inverter control.

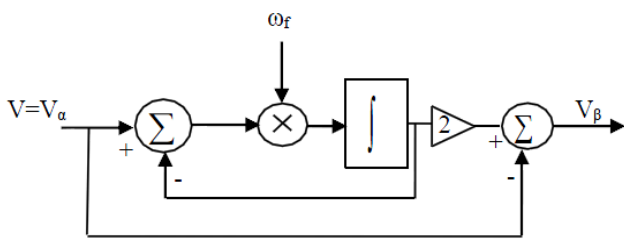


Fig. 5. All pass filter (APF)

### VI. CONTROLLER DESIGN

The control structure consists of a synchronous reference frame proportional integral controller (SRFPI) to control the instantaneous output voltage, and an inner capacitor current loop to produce a sinusoidal capacitor current and hence reduce the disturbances produced due to nonlinear current. Instead of conventional inductor current loop, here a capacitor current inner loop is used as it is easier to sense, considering the low magnitude and it gives better disturbance rejection compared to former technique. The current reference for the capacitor current loop is generated from the SRFPI outer loop. In the proposed control strategy, the inner current loop gain is obtained considering the bandwidth of operation required for the varying load conditions. The proper selection of the proportional gain of the loop enables a perfect blocking of load disturbances and an instantaneous dynamic response. The proportional and integral gain for the outer loop is now calculated considering the chosen value for inner current loop gain.

#### A. INNER CURRENT LOOP

The simplified block diagram of the inner current loop control is shown in the fig. 6.

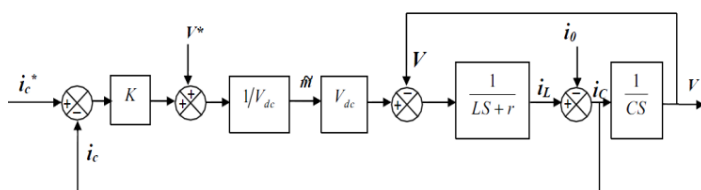


Fig. 6. All pass filter (APF)

Here the  $I_c^*$  is obtained from the outer control scheme. Assuming the load impedance as  $Z$  and deriving the transfer function of the block considering  $I_c$  as the output we get (9).

$$G(s) = \frac{i_c}{i_c^*} = \frac{CZKs}{LCZs^2 + (CZ(r+K) + L)s + r} \quad (9)$$

The value of  $K$  is chosen as per the bandwidth requirement of the inner current loop. The bandwidth in turn is a function of the load impedance, so based on the range of expected variation of the inverter load, proper value of the bandwidth must be set. A perfect rejection of the load disturbance and instantaneous dynamic output response is obtained for a bandwidth closer to the PWM switching frequency but this increases the system response to the switching noises. In practice values close to quarter of the PWM frequency is employed as the bandwidth of the inner loop. This value comes as  $\omega_{bi} = 25$  krad/s. The value of optimum gain can be obtained by substituting values of the available parameters and solving for  $K$  taking  $G(j\omega_{bi}) = 0.5$ , which comes as 16.

#### B. OUTER LOOP

The inner current loop gets the reference current from the outer SRFPI controller. Therefore, the outer loop transfer function consists of the transfer function of the SRFPI controller,  $H(s)$  combined with the inner loop transfer function. The block diagram and simplified form is shown in fig. 7.

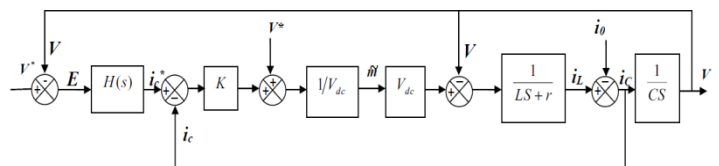


Fig. 7. Block diagram of outer loop

As already specified, the value of reference current used in the inner control loop is derived from the SRFPI outer loop. The transforming equation in matrix form is illustrated in (10)

$$\begin{bmatrix} i^*_{C,\alpha}(t) \\ i^*_{C,\beta}(t) \end{bmatrix} = \begin{bmatrix} \cos(\omega_f t) & -\sin(\omega_f t) \\ \sin(\omega_f t) & \cos(\omega_f t) \end{bmatrix} \begin{bmatrix} G_{PI}(t) & 0 \\ 0 & G_{PI}(t) \end{bmatrix} * \begin{bmatrix} \cos(\omega_f t) & \sin(\omega_f t) \\ -\sin(\omega_f t) & \cos(\omega_f t) \end{bmatrix} \begin{bmatrix} E_{\alpha}(t) \\ E_{\beta}(t) \end{bmatrix} \quad (10)$$

Here  $G_{PI} = K_p + K_i/S$ , is the proportional integral controller function. The function E is obtained from the arithmetic difference between the synchronous reference voltage fed to the outer loop and the filter capacitance voltage.

The overall transfer function of the control system, assuming a lightly loaded condition wherein the load impedance Z tends to be very high is given by (11).

$$\frac{V}{V^*} = \frac{K(a_3 s^3 + a_3 s^2 + a_3 s + a_3 0)}{LC s^5 + bs^4 + (b\omega_f + Ka_3)s^3 + (b\omega_f^2 + Ka_2)s^2 + ((r+K)C\omega_f^3 + Ka_1)s + Ka_0} \quad (11)$$

Where,  $a_3 = K_p$ ,  $a_2 = K_p \omega_f + K_i$ ,  
 $a_1 = K_p \omega_f^2 + 2\omega_f K_i$ ,  $a_0 = K_p \omega_f^3 - K_i \omega_f^2$ ,  $b = (L\omega_f + r + K)C$

The selection of proportional gain determines both the maximum voltage regulation bandwidth and the system stability, whereas the minimum steady state error is ensured by proper value of the integral gain.

The value of  $K_p$ , is determined assuming negligible effect of  $K_i$ . This value sets the transient and steady state response of system to be depended only on value of  $K_i$ . Taking the above condition the (11) is rewritten as (12).

$$\frac{V}{V^*} \cong \frac{K_p K}{K_p K - LC\omega^2 + j(r+K)C\omega} \quad (12)$$

The bandwidth  $\omega$  for inverter application in (12) is fixed considering the transient response and noise

rejection capability. For the application of inverter under study the value of bandwidth is taken as 8 krad/s. Having got the value of K from inner loop design and substituting the values of known parameters the value for  $K_p$  for the outer control loop can be obtained as 0.15. The value of integral gain  $K_i$  is now finalized by applying Routh Hurwitz stability criterion to the characteristic equation of closed loop control scheme obtained from (11) using the stability constraint we get the upper limit for the integral gain defined by  $K_i < K_p * \omega_f$ . For our application the value is given by  $K_i < 55$ . A high value for integral gain ensures high overall gain for the system, whereas it causes the interference with other frequencies. Assuming a mean value we take the integral gain as 30.

## VII. RESULTS

The required PV fed inverter is simulated with different types of loads and the THD is calculated in each step to make sure it is apt for the critical load application required by the UPS. The simulation results of the single phase inverter control with RL load is shown in fig. 8. It can be seen that the voltage and current waveforms are purely sinusoidal. The values of peak voltage and current are mentioned along with their waveforms. The total harmonic distortion is obtained as 0.36 percent as shown in fig 9. Simulation results for a diode bridge rectifier connected at the load end of inverter are shown in fig.10. It can be seen that the voltage at the output terminal of the inverter for the diode bridge rectifier load is somewhat distorted. But THD analysis has revealed that the values are 4.24 percent, which is within the permissible limits as shown in fig.11. Similarly load voltage and current for an Ac voltage controller is shown in fig.12. Here we can see distortion in voltage and current due to the switching transients, for the mosfet present in the circuit of AC voltage controller. The THD is found to be 4.49 percent as shown in fig.13.

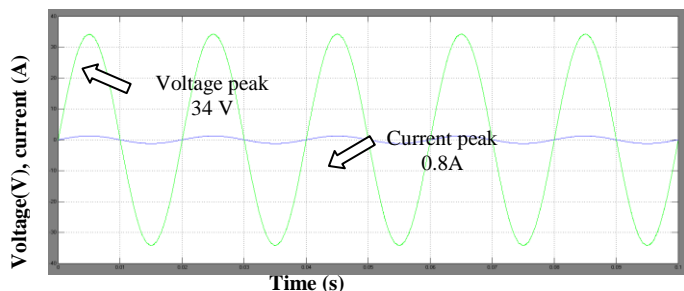


Fig. 8. Simulation output with RL load

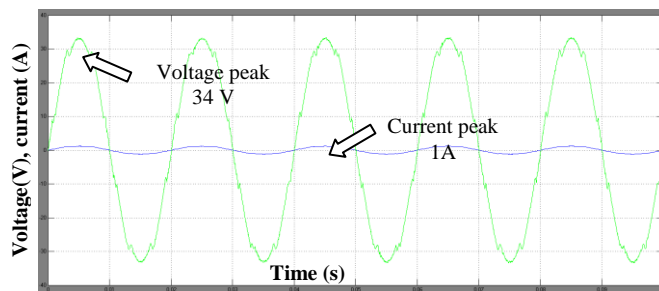


Fig. 12. Simulation output with non linear load – Ac voltage controller.

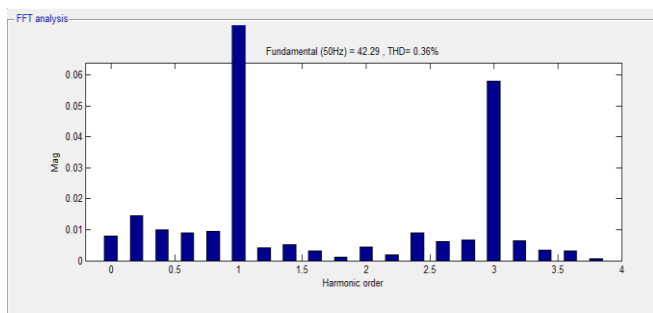


Fig. 9. THD analysis of Inverter with RL load

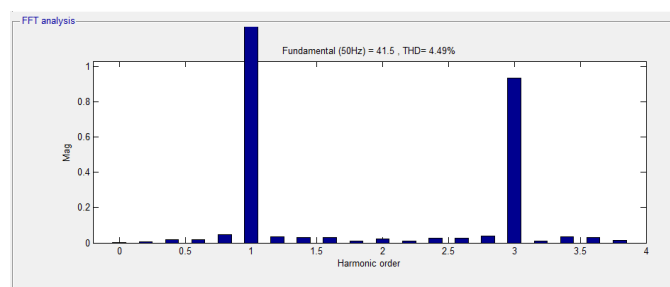


Fig. 13. THD analysis of Inverter with AC voltage regulator at its load

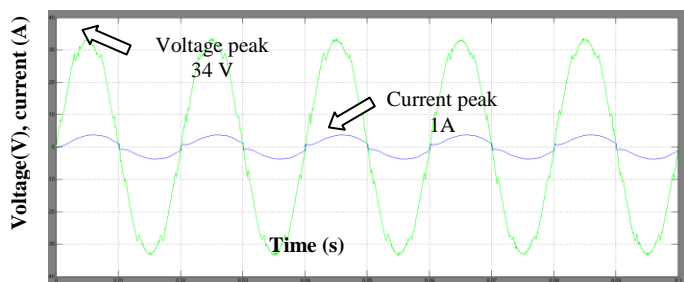


Fig. 10. Simulation output with non linear load – Uncontrolled rectifier.

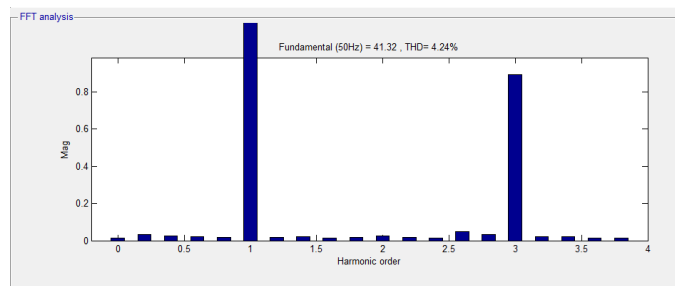


Fig.11. THD analysis of Inverter with uncontrolled rectifier as load

## VIII. CONCLUSIONS

Hence the inverter for UPS application fed from a PV module is designed and analysed with Matlab simulations. The design equations are presented for the control strategy. The simulation results for the power circuit designed with the control strategy are presented, which verifies the compatibility of inverter under different types of loads connected at its terminals.

## REFERENCES

- [1] Y.Xue, L. Chang, S.B. Kjaer, J. Bordonau, and Toshihisa Shimizu, "Topologies of Single-Phase Inverters for Small Distributed Power Generators: An Overview," IEEE Transactions on Power Electronics, vol. 19, pp. 1305-1314, Sept. 2004
- [2] S. B. Kjaer, J. K. Pedersen, and F. Blaabjerg, "A review of single-phase grid-connected inverters for photovoltaic modules," IEEE Trans. Ind. Appl., vol. 41, no. 5, pp. 1292-1306, Sep./Oct. 2005.
- [3] C. G. C. Branco, R. P. Torrico-Bascope, C. M. T. Cruz, and F. K. de A Lima, "Proposal of three-phase high-frequency transformer isolation UPS topologies for distributed generation applications," IEEE Trans. Ind. Electron., vol. 60, no. 4, pp. 1520-1531, Apr. 2013.
- [4] M. Calais, J. Myrzik, T. Spooner, and V. G. Agelidis, "Inverters for singlephase grid connected photovoltaic systems—An overview," in Proc. IEEE PES, 2002, vol. 4, pp. 1995-2000.

- [5] K. Zhou, K. Low, D. Wang, F. Luo, B. Zhang, and Y. Wang, "Zero-phase odd-harmonic repetitive controller for a single-phase PWM inverter," *IEEE Trans. Power Electron.*, vol. 21, no. 1, pp. 193–201, Jan. 2006.
- [6] S. Buso, S. Fasolo, and P. Mattavelli, "Uninterruptible power supply multiloop control employing digital predictive voltage and current regulators," *IEEE Trans. Ind. Appl.*, vol. 37, no. 6, pp. 1846–1854, Nov./Dec. 2001.
- [7] H. Komurcugil, "Rotating-sliding-line-based sliding-mode control for single-phase UPS inverters," *IEEE Trans. Ind. Electron.*, vol. 59, no. 10, pp. 3719–3726, Oct. 2012.
- [8] T. L. Tai and J. S. Chen, "UPS inverter design using discrete-time sliding mode control scheme," *IEEE Trans. Ind. Electron.*, vol. 49, no. 1, pp. 67–75, Feb. 2002.
- [9] R. Zhang, M. Cardinal, P. Szczesny, and M. Dame, "A grid simulator with control of single-phase power converters in D-Q rotating frame," in *Proc. IEEE Power Electron. Spec. Conf.*, 2002, pp. 1431–1436.
- [10] A. Roshan, R. Burgos, A. C. Baisden, F. Wang, and D. Boroyevich, "A D-Q frame controller for a full-bridge single phase inverter used in small distributed power generation systems," in *Proc. IEEE APEC*, Feb. 2007, pp. 641–647.
- [11] M. Saitou and T. Shimizu, "Generalized theory of instantaneous active and reactive powers in single-phase circuits based on Hilbert transform," in *Proc. 33rd Annu. IEEE PESC*, Jun. 2002, pp. 1419–1424.
- [12] K. De Brabandere, T. Loix, K. Engelen, B. Bolsens, J. Van den Keybus, J. Driesen, and R. Belmans, "Design and operation of a phase-locked loop with Kalman estimator-based filter for single-phase applications," in *Proc. IEEE Ind. Electron. Soc. Conf.*, 2006, pp. 525–530.
- [13] R. Y. Kim, S. Y. Choi, and I. Y. Suh, "Instantaneous control of average power for grid tie inverter using single phase D-Q rotating frame with all pass filter," in *Proc. IEEE Annu. Conf. Ind. Electron. Soc.*, Nov. 2004, pp. 274–279.
- [14] A single-stage, single-phase, transformer less, doubly grounded grid connected PV system, Hiren Patel and Vivek Agarwal, Senior member IEEE